Response versus Chain Length of Alkanethiol-Capped Au Nanoparticle Chemiresistive Chemical Vapor Sensors

ARTICLE *in* THE JOURNAL OF PHYSICAL CHEMISTRY C · DECEMBER 2010

Impact Factor: 4.77 · DOI: 10.1021/jp101331g · Source: OAI

Response versus Chain Length of Alkanethiol-Capped Au Nanoparticle Chemiresistive Chemical Vapor Sensors

Edgardo García-Berríos,[†] Ting Gao,[†,‡] Marc D. Woodka,[†] Stephen Maldonado,[§] Bruce S. Brunschwig,[∥] Mark W. Ellsworth,[‡] and Nathan S. Lewis*[,†]

Noyes Laboratory 210, 127-72, Division of Chemistry and Chemical Engineering, California Institute of Technology, Pasadena, California 91125, Polymer, Ceramics, and Technical Services Laboratories, Tyco Electronics Corporation, Technology Group, 306 Constitution Drive, Menlo Park, California 94025, Department of Chemistry, University of Michigan, Ann Arbor, Michigan 48109, and Beckman Institute, California Institute of Technology, Pasadena, California 91125

Received: February 11, 2010; Revised Manuscript Received: August 12, 2010

Au nanoparticles capped with a homologous series of straight chain alkanethiols (containing 4−11 carbons in length) have been investigated as chemiresistive organic vapor sensors. The series of alkanethiols was used to elucidate the mechanisms of vapor detection by such capped nanoparticle chemiresistive films and to highlight the molecular design principles that govern enhanced detection. The thiolated Au nanoparticle chemiresistors demonstrated rapid and reversible responses to a set of test vapors (*n*-hexane, *n*-heptane, *n*-octane, iso-octane, cyclohexane, toluene, ethyl acetate, methanol, ethanol, isopropanol, and 1-butanol) that possessed a variety of analyte physicochemical properties. The resistance sensitivity to nonpolar and aprotic polar vapors systematically increased as the chain length of the capping reagent increased. Decreases in the nanoparticle film resistances, which produced negative values of the differential resistance response, were observed upon exposure of the sensor films to alcohol vapors. The response signals became more negative with higher alcohol vapor concentrations, producing negative values of the sensor sensitivity. Sorption data measured on Au nanoparticle chemiresistor films using a quartz crystal microbalance allowed for the measurement of the partition coefficients of test vapors in the Au nanoparticle films. This measurement assumed that analyte sorption only occurred at the organic interface and not the surface of the Au core. Such an assumption produced partition coefficient values that were independent of the length of the ligand. Furthermore, the value of the partition coefficient was used to obtain the particle-to-particle interfacial effective dielectric constant of films upon exposure to analyte vapors. The values of the dielectric constant upon exposure to alcohol vapors suggested that the observed resistance response changes observed were not significantly influenced by this dielectric change, but rather were primarily influenced by morphological changes and by changes in the interparticle spacing.

I. Introduction

Sensor arrays have attracted significant interest due to their ability to classify and quantitate analytes in liquid and gaseous environments.[1] Chemiresistive thin films comprised of an insulating organic polymer or small molecule material combined with electronically conductive carbon black particles are attractive because such sensors are low power and are broadly responsive to a variety of analytes.[2−4] Chemiresistive composite sensors generally operate via a volumetric sensing modality wherein a vapor-induced volumetric expansion of the film produces a reversible change in the DC resistance of the film.[2] Sensor films of Au nanoparticles (Au-NPs) capped with organothiol ligands have also been investigated.[5−7] Organically capped metal nanoparticles consist of a small metal core (typically less than 10 nm in diameter) surrounded by a dense organic layer of insulating material that is used to chemically protect the metal particles. These materials, with an approximate stoichiometry of 3:1 (Au/S-R), are easily synthesized using wet chemical techniques and can remain soluble for extended periods in common organic solvents.[8−10]

Sensors can be prepared by the deposition of a thin film of the Au-NPs between two metal electrodes. Measurement of the resistance of the film provides a facile method for transduction of the sorption of organic vapor into a detectable electrical signal. As opposed to conventional polymer/carbon black composites, in which the insulating matrix and conducting species are in physical contact, capped Au-NPs have both constituents chemically bound together. Generally, in such sensors, the amount of analyte sorbed by the film is negligible compared with the amount of material in the organic phase.

Upon exposure to organic vapors, analyte partitions into the film, effecting changes in the electrical conductivity of the film through changes in the film's morphology (e.g., in the film swelling through changes in the interparticle spacing) or in the physical properties of the film, such as its dielectric constant. In the majority of cases, swelling predominates and the resistance of the film increases upon exposure to an analyte; however, in some cases, decreases in resistance have been observed upon exposure to certain analytes.

* To whom correspondence should be addressed. Phone: 626-395-6335. Fax: 626-395-8867. E-mail: nslewis@caltech.edu.
[†] Division of Chemistry and Chemical Engineering, California Institute of Technology.
[‡] Tyco Electronics Corporation.
[§] University of Michigan.
[∥] Beckman Institute, California Institute of Technology.

10.1021/jp101331g
Published on Web 08/25/2010

Au-NP sensors have been studied (e.g., electric resistance, resonator frequency change) using Au-NPs capped with alkanethiols,[7,11] dithiols,[12−15] π-conjugated thiols,[16−19] hydroxy- and carboxylic-terminated alkanethiols,[12] carboxylic−metal−carboxylic ligands,[20] dendrimers,[13,21−23] and mixture of ligands,[24] as well as other ligands.[25−27] Wohjtlen and Snow introduced these materials as chemical sensors using octanethiol-capped Au-NPs.[7] Increases in the electrical resistance were observed when the sensors were exposed to toluene or tetrachloroethylene vapors. Surprisingly, for hydrophilic vapors such as 1-propanol, ethanol, and water, a decrease in the electrical resistance was observed when long chain alkanethiols were used as capping ligands.[11]

Guo et al. demonstrated that, when alkanethiol-capped Au-NP films that contained traces of the phase-transfer reagent tetraoctylammonium bromide (TOABr) used in the Au-NP synthesis[8] were used as chemiresistive sensors, the film resistance decreased when the sensors were exposed to water vapor.[28] Ibañez et al. observed decreases in resistance when a film composed of TOABr-functionalized Au-NPs was exposed to methanol, ethanol, isopropanol, or toluene.[29] The ability to control the sign of the sensor response to an analyte by use of different phase-transfer reagents would add unique capabilities to arrays of such sensors and would therefore significantly increase their ability to identify or classify vapors.

The electronic conductivity of the organothiol capped Au-NP films is the result of electrons hopping between Au-NP centers in the film. Empirically, the conductivity of a film, σ, can be described by

$$\sigma = \sigma_0 \exp(-A/k_B T) \tag{1}$$

where σ_0 and A are constants. Initially, the hopping was described by granular metal theory, with A interpreted as an activation energy associated with the creation of a positive and negative pair of NPs from two NPs.[30,31]

More recently, Murray and co-workers[24,32−39] have described the hopping as the transfer of an electron from a negative (or neutral) Au-NP site to a neighboring neutral (or positive) Au-NP site. This view treats each hop as equivalent to an electron exchange in a mixed valence system. Thus, for conduction by this method, both oxidized (or reduced) and neutral Au-NP sites must exist in the film. For neutral Au-NP films, the mixed valence sites could be produced by spontaneous disproportionation

$$2[\text{Au}-\text{NP}] \rightarrow [\text{Au}-\text{NP}]^+ + [\text{Au}-\text{NP}]^-$$

Electron-exchange has been theoretically described by Marcus.[40] In this approach, the prefactor σ_0 is related to the coupling between the two centers, and is dependent on distance with a form of

$$\sigma_0 = \sigma^0 \exp[-(2a - r)\beta] \tag{2a}$$

where σ^0 is the maximum conductance for particles that are separated by a distance $2a$, and a is the radius of the NP. In this framework, the value of A in eq 1 is interpreted as arising from the reorganizational barrier that results from the requirement that the electron-transfer pair reorganize to a nuclear configuration that is energetically degenerate for the electron on either center. Thus, A is given by

$$A = \lambda/4 \tag{2b}$$

where λ is the reorganization energy for the electron exchange process. The reorganization energy is primarily the result of the polarization of the medium by the charged centers, and for particles separated by $2a + \delta$, λ is given by

$$\lambda = \frac{e^2}{4\pi\varepsilon_0}\left(\frac{1}{a} - \frac{1}{2a + \delta}\right)\left(\frac{1}{\varepsilon_{op}} - \frac{1}{\varepsilon_s}\right) \tag{3}$$

where ε_o is the permittivity of free space, and ε_{op} and ε_s are the optical and static dielectric permittivity of the medium, respectively.[40,41] Murray has advanced a series of arguments in favor of the mixed-valence type of electron hopping dominating the transport in such films.

In this work, we have explored the effect of changing the length of the Au-NP capping alkanethiol (R-SH) on the performance of such films as chemical vapor sensors by investigating the response sensitivity to a variety of vapors. We have also investigated the influence of the physicochemical properties of sorbed analyte on the relative differential resistance response of the Au-NP film by using a dielectric constant model for mixtures of two components (e.g., capping ligand and the sorbed analyte). The relative differential resistance response values were compared to the dielectric constant change produced by analyte sorption, to elucidate whether negative responses arise from a dielectric change or other extrinsic film components. Information about the amount of analyte material sorbed at the Au-NP films was obtained by using the partition coefficient of the sensor-analyte combination as determined by quartz crystal microbalance (QCM) measurements. The determination of the partition coefficients of the Au-NP films assumed that analyte sorption occurred at the organic ligand, and that zero or negligible sorption occurred at the metal core. The response values as a function of temperature have also been investigated.

II. Experimental Section

A. Materials. Sodium borohydride ($NaBH_4$, 99%), hydrogen tetrachloroaurate trihydrate ($HAuCl_4 \cdot 3H_2O$, ACS reagent), tetraoctylammonium bromide (TOABr, ≥ 99%), 1-butanethiol (99%), 1-pentanethiol (98%), 1-hexanethiol (97%), 1-heptanethiol (98%), 1-octanethiol (98.5%), 1-nonanethiol (95%), 1-decanethiol (96%), 1-undecanethiol (98%), and the test analytes (*n*-hexane, *n*-heptane, *n*-octane, iso-octane, cyclohexane, toluene, ethyl acetate, methanol, ethanol, isopropanol, and 1-butanol) were obtained from Aldrich Chemical Corp, except for 1-hexanethiol (97%), which was obtained from Alfa Aesar. All of the reagents and solvents were used without further purification. The 18 MOhm-cm resistivity deionized water was obtained from a Barnstead Nanopure purification system.

Au-NPs capped with R-S functionality were synthesized as described by Brust et al.,[8,42] with the use of TOABr. Briefly, 4.56 g of TOABr was dissolved in 165 mL of toluene in a 1000 mL round-bottom flask. A solution containing 0.8025 g of $HAuCl_4 \cdot 3H_2O$ dissolved in 60 mL of deionized water was then added. The resulting dark-red biphasic mixture was stirred vigorously while a solution that contained one equivalent of organothiol in 10 mL of toluene was added. Finally, a solution of 0.787 g $NaBH_4$ dissolved in 55 mL of water was added dropwise over 300 s to the vigorously stirred solution. During the addition of $NaBH_4$, the mixture turned dark purple. After stirring for 3 h, the organic phase was separated, transferred to a separatory funnel, and rinsed with water. The soluble product remaining in the organic phase was concentrated by rotary evaporation to a volume of ~10 mL and was precipitated in

800 mL of ethanol at 10 °C. After settling overnight, the clear supernatant was decanted and the settled product was collected by centrifugation, followed by a wash with fresh ethanol. The product was redissolved in 10 mL of toluene and then reprecipitated by dropwise addition into 200 mL of rapidly stirred ethanol. After settling overnight at 10 °C, the 200 mL suspension was centrifuged. The precipitate was washed with fresh ethanol, vacuum-dried, and redissolved in toluene (10 mg/mL). The Au atom to ligand ratio, Au/S-R, was determined by thermogravimetric analysis to be 3(±0.1):1 (Figure S1), and transmission electron microscopy indicated that the metal core had a diameter of approximately 2 (±1) nm. The solution was stored at 10 °C until needed. The capped Au-NPs are referred to as Au-Cn ($4 \leq n \leq 11$).

NP films were prepared on 1 × 2 cm glass substrates with metal contacts in the form of gold interdigitated electrodes (IDEs; 50 nm of Au over 30 nm of Cr). The electrode pattern produced 20 parallel sets of IDEs, with each IDE having dimensions of 0.240 mm × 5 mm ($w \times l$), separated by a 10 μm gap. The NP films were cast from a sonicated solution (10 mg/mL in toluene) by manually depositing a 10 μL suspension directly over the region of the substrate that contained the IDEs. Care was taken to ensure that deposition of the films was performed on substrates that were maintained below the decomposition temperature of the capped colloidal sensor materials.

For capping agents longer than eight carbon units, the 10 μm gap between the electrodes was not sufficiently small to yield reproducible measurable film resistances. For shorter units such as propanethiol-capped NPs, dilution was very difficult, producing irreproducible electrical resistances. The stability of these NPs was observed to be low, leaving yellowish gold clusters on the glassware used. For all the sensors discussed herein, well-dispersed solutions were obtained and sensor film resistances were reproducible.

B. Sensing Measurements. Typically, three nominally identical vapor sensors were prepared at a time. The sensors were loaded into a rectangular, 40-slot chamber, with sensor film replicates positioned randomly. No dependence was observed on the performance of a given sensor on its spatial position in the array. The 45.5 × 3.0 × 1.5 cm ($w \times l \times d$) chamber was connected by Teflon tubing to the gas delivery system. The internal cross-sectional area of the chamber was 1 cm^2. The dc resistance of the sensor array was measured with a digital multimeter (Keithley Model 2002) connected to a multiplexing unit (Keithley Model 7001). The resistance data were collected every 5−7 s from the array. A computer-controlled (LabVIEW) flow system delivered pulses of analyte vapor at a given fraction of the analyte's vapor pressure.[43] Oil-free air was obtained from the house compressed air source (1.10 ± 0.15 ppth of water vapor) controlled with a mass flow controller. The test analytes used were six hydrocarbons (*n*-hexane [Hex], *n*-heptane [Hept], *n*-octane [Oct], iso-octane [*i*Oct], cyclohexane [*c*Hex], and toluene [Tol]), four alcohols (methanol [MeOH], ethanol [EtOH], isopropanol [*i*POH], and 1-butanol [BuOH]), and ethyl acetate [EtOAc]. The sensor response as a function of vapor concentration was studied over the concentration range that corresponded to $0.0010 \leq P/P^\circ \leq 0.0200$, where P and P° are the partial pressure and vapor pressure of the analyte at room temperature (22 °C), respectively. Table 1 shows the saturated vapor pressures (P°, ppm) and the static dielectric constants, ε_s, of the analytes used.[44] Each analyte presentation consisted of 70 s of air, followed by 80 s of analyte vapor, followed by 60 s of air to purge the system. The total flow rate for each analyte presentation was 5 L min^{-1}. For the resistance and QCM sensitivity measurements, three exposures at each P/P° (see Table 1) were performed.

TABLE 1: Saturated Vapor Pressure, P° (ppm), and Dielectric Constant, ε_s at 22 °C for All Analytes Used

	P° (× 10^{-4})	ε_s
Hex	17.4	1.89
Hept	5.11	1.92
Oct	1.54	1.95
*i*Oct	5.58	1.94
*c*Hex	11.3	2.02
Tol	3.17	2.38
EtOAc	1.05	6.02
MeOH	14.1	32.7
EtOH	6.51	24.6
*i*POH	4.93	20.2
BuOH	0.733	17.8

For resistance measurements as a function of the sensor temperature, the sensor chamber (sealed with plastics and Teflon) was placed in a water bath whose temperature was controlled with a Haake K20/DC5 temperature controller. Only three sensors (Au−C6, Au−C7, and Au−C8) were placed in the chamber. During the stabilization of the desired temperature (2 h) an air background flow was continuously exposed to the array.

QCM measurements were performed using quartz substrates with a 10 MHz resonant frequency and a diameter of 13.7 mm. The frequency was monitored using a Hewlett-Packard Frequency Counter (Model HP 53181a, 225 MHz), with an aluminum/Teflon chamber of dimensions 8.5 × 6.0 × 3.0 cm ($w \times l \times d$). NP films were deposited on the substrates by spraying using an airbrush. Two nominal QCM sensors were used for each Au−C*n* system investigated.

For optical measurements of the Au−NP plasmon resonance spectra, a Au−NP film was deposited on glass and placed in a sealed Teflon cylindrical chamber that permitted vapor flow through two apertures (inlet and outlet). The volume of the chamber was approximately 100 mL. The spectra were obtained with an Agilent 8453 UV−visible spectrometer.

All chemiresistive and QCM sensors were dried under vacuum for 30 min at room temperature. The sensor films were conditioned by analyte exposures for 80 h to reach a steady resistance or frequency baseline, prior to the data collection presented herein.

C. Data Processing. All data processing was carried out using MATLAB[45] with custom written routines.

i. Chemiresistive Sensors. The resistance-based response, r_s, of a vapor sensor to a particular analyte was calculated as $r_s = \Delta R_{max}/R_b$, where R_b is the baseline-corrected resistance of the sensor in the absence of analyte, and ΔR_{max} is the baseline-corrected maximum resistance change upon exposure of the sensor to analyte. R_b values were obtained from fitting a line to the pre-exposure data and extrapolating over the exposure period (see Figure S2). ΔR_{max} was the average of the maximum three readings obtained by subtracting R_b from the measured sensor resistance during the exposure time. Prior studies have shown that $\Delta R_{max}/R_b$ is a more reproducible metric than ΔR_{max}.[27,46] The sensitivity of a resistance-based vapor sensor film, s_R, was calculated from the slope of r_s versus P/P°, using a linear least-squares fit.

ii. QCM Sensors. The frequency of the QCM crystal was measured before, f_0, and after deposition of the sensor film, f_f, and after exposure to analyte, f_a. The change in frequency for the QCM crystal upon exposure to analyte was measured using analogous methods to that used for the change in resistance.

The change in frequency is directly proportional to the increase in mass of the crystal. Thus, for the film prior to exposure to analyte, $\Delta f_f = f_f - f_0 = Cm_f$, and after exposure, $\Delta f_a = f_a - f_f = C\Delta m_f$, where C is a constant, m_f is the mass of the film, and Δm_f is the increase in mass of the film on exposure to analyte.[47] Assuming that only the thiol ligands and not the metal core sorb analyte, the observed frequency change due to the application of the sensor film to the QCM crystal, Δf_a, was corrected to account for the mass change due to only the proportion of the film that was comprised of the organic ligands. Thus, Δf_a was adjusted by the relative mass fraction of organic ligand that was obtained from the Au/S-R ratio (3:1):

$$\Delta f_f' = f_{ligand}\Delta f_f \quad (4)$$

where f_{ligand} is the mass fraction of thiol ligand in the NP film. The relative mass increase due to analyte sorbed per unit mass of sensor material, r_{QCM}, is then given by

$$r_{QCM} = \frac{\Delta f_a}{\Delta f_f'} = \frac{\Delta m_a}{m_1} \quad (5)$$

where m_l is the mass of the organic ligands in the film.

Random exposures of the analytes were presented to the Au-NP QCM sensors. The QCM sensitivity, s_{QCM}, was calculated from the slope of r_{QCM} versus $P/P°$ using a linear least-squares fit, with a forced zero intercept. Partition coefficients, K, incorporating responses for $0.0010 \leq P/P° \leq 0.0200$, were obtained as described previously by[48]

$$K = \frac{\rho_s RT}{M_{w,A}P°}s_{QCM} \quad (6)$$

where ρ_s (g cm^{-3}) is the density of the sorption material (R-SH), R (atm mol^{-1} K^{-1}) is the ideal gas constant, T (K) is the temperature, $M_{w,A}$ (g mol^{-1}) is the molecular weight of the analyte, and $P°$ (atm) is the vapor pressure of the analyte. The density of the sorption material, ρ_s, was taken as that of the R-SH ligands (0.84 g cm^{-3}), assuming that the change in density of the ordered ligands on the surface was negligible.

III. Results

A. Resistance Change Response to Analytes. Typical sensor responses, r_s, for a Au−C8 sensor to Hex and EtOH at $P/P° = 0.0050$ are shown in Figure 1a and b, respectively. Positive responses (resistance increases) were observed for all sensors upon exposure to the hydrocarbons or to EtOAc, whereas negative responses (resistance decreases) were observed upon exposure to alcohol vapors. The positive responses of the sensors to EtOAc were significantly smaller than the responses observed upon exposure to the hydrocarbon analytes. Au-NP films showed no change in the amount of organic material before and after the sensing experiments, as determined by thermogravimetric analysis.

The sensor response as a function of analyte concentration was generally linear over the $P/P°$ range investigated. Emphasis was placed on measurement of and understanding of the response to relatively dilute analytes, because most situations of interest are likely to involve lower, rather than higher, concentrations of vapor at the position of the sensor itself. Figure S3 shows a linear least-squares fit for a Au−C8 sensor against

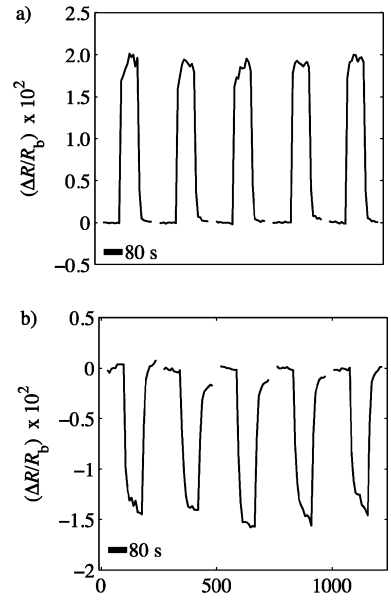

Figure 1. Relative differential resistance values, $\Delta R/R_b$, for five different randomly ordered exposures to hexane and ethanol, each at $P/P° = 0.0050$: (a) hexane exposures to a Au−C8 vapor sensor; (b) ethanol exposures to a Au−C8 vapor sensor.

all of the 11 vapors, with the sensor sensitivity given as the slope, s_R, of the best fit straight line. The fits for the hydrocarbon and EtOAc responses gave nonzero positive intercepts, C, having a value of $\Delta R_{max}/R_b$ between (1.3 and 0.4) $\times 10^{-2}$. For all of the alcohols except EtOH, a zero intercept was observed, whereas for EtOH vapors, a negative intercept was observed. The responses generally became nonlinear functions of analyte vapor for $P/P° > 0.1$. The sensor sensitivity generally increased as the length of the R-SH capping chain increased (Figure 2). The sensitivities for *i*POH and BuOH were essentially the same for the Au−C7 and Au−C8 NP films.

Figure 3 shows the responses to Hex and EtOH as a function of temperature (4 °C $\leq T \leq$ 39 °C) for a Au−C8 sensor. The arrows show the direction of the temperature scan, with the initial scan starting at the lowest temperature. Each r_s value was the average of 50 exposures per analyte. For Hex, r_S decreased as the temperature increased, in accord with changes in the value of $P/P°$ due to an increase in the value of $P°$ as the temperature increased (see Table S1). Upon exposure to Hex, the r_S values were slightly smaller during the reverse temperature scan than those in the increasing temperature scan. Negative responses were observed for a Au−C8 sensor upon exposure to EtOH during the forward temperature scan. However, for the backward temperature scan, positive values of r_s were observed.

B. QCM Response to Analytes. Figure 4 shows the QCM frequency changes for a Au−C8 sensor upon exposure to Hex or EtOH at $P/P° = 0.0050$. The QCM sensitivities, s_{QCM}, were obtained from the linear least-squares slope of a plot of r_{QCM} versus $P/P°$ (Figure 5). In all cases, s_{QCM} values were positive and showed no significant dependence on the chain length of the capping ligand. Furthermore, the values of K were generally independent of chain length (Figure 6). This behavior is expected because the calculation of r_{QCM}, eq 5, used a film mass that was only the mass of the organic ligands. If the sorption of analyte is only performed by the organic ligands, then the values of r_{QCM} should be independent of the length of the ligands. This behavior would also produce a lack of dependence of s_{QCM} or K on the length of the capping alkane chain.

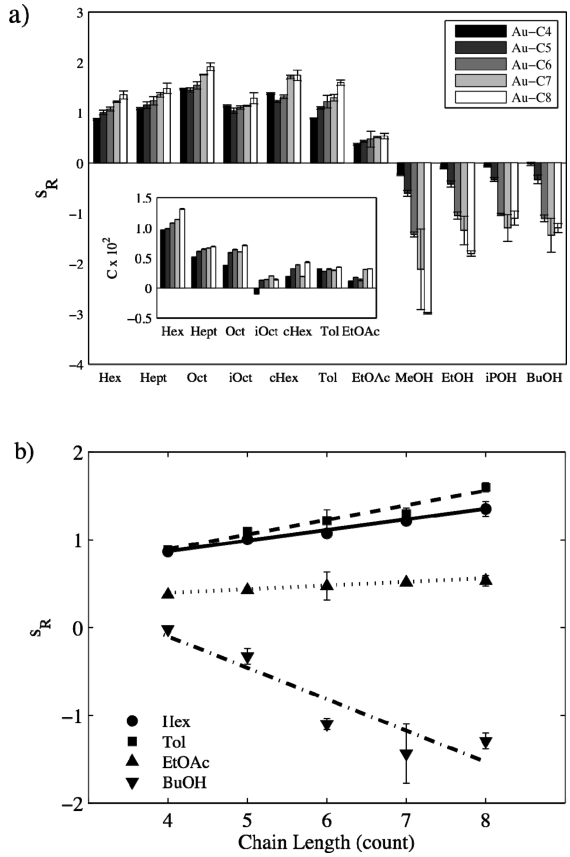

Figure 2. (a) Resistance-based sensitivity values, s_R, for all combinations of alkanethiol-capped Au nanoparticles and analytes, for $0.0010 \leq P/P^\circ \leq 0.0200$. Each value represents the average of three sensor replicates for every Au−C*n* capping ligand. The inset shows the values of the intercept, *C*, obtained upon exposure to the hydrocarbons. (b) Resistance-based sensitivity, s_R, as a function of chain length (Au-Cn; $4 \leq n \leq 8$) of the Au-capping alkanethiol. The s_R values presented correspond to *n*-hexane (Hex), toluene (Tol), ethyl acetate (EtOAc), and 1-butanol (BuOH).

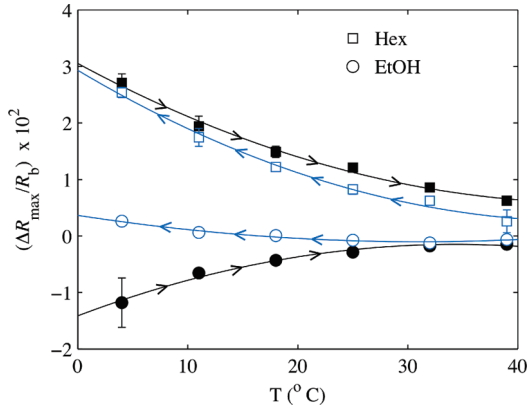

Figure 3. Maximum relative differential resistance responses for a Au−C8 sensor upon exposure to Hex (squares) and EtOH (circles) at $P/P^\circ = 0.0010$, as a function of temperature ($4\ ^\circ\text{C} \leq T \leq 39\ ^\circ\text{C}$). The arrows in the response pattern represent the direction of the temperature scan. The responses observed as the temperature was increased (black) were generated initially, followed by the blue-line scan for decreases in temperature. Each response value was the average of 50 exposures per analyte.

IV. Discussion

The use of different capping ligands with different lengths allows for control at the molecular level over the interparticle spacing, and the mass of the spacing ligands in the sensor films.

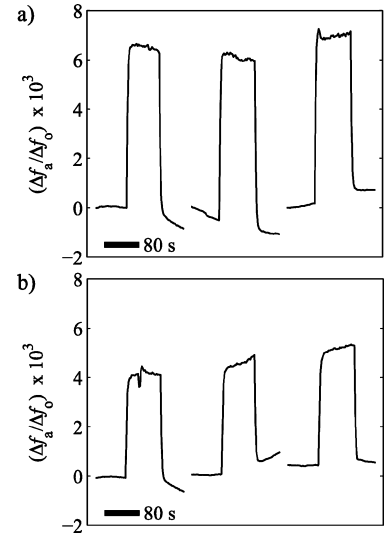

Figure 4. QCM sensor responses for a Au−C8 film upon exposure to (a) hexane and (b) ethanol, each at $P/P^\circ = 0.0050$.

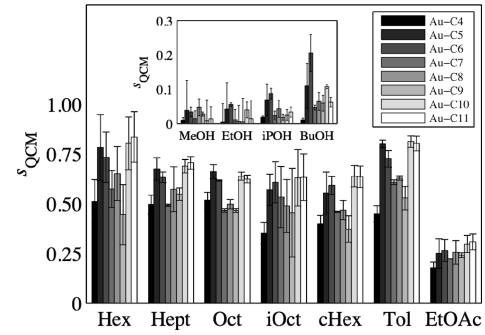

Figure 5. Quartz crystal microbalance sensitivity, s_{QCM} (Hz ppm^{-1} $\times$ 10^1) for all combinations of capped Au nanoparticle sensors and analytes, for $0.0010 \leq P/P^\circ \leq 0.0200$. Each value corresponds to the average of two sensors per Au−C*n*. The inset shows the adjusted s_{QCM} values for alcohol vapors.

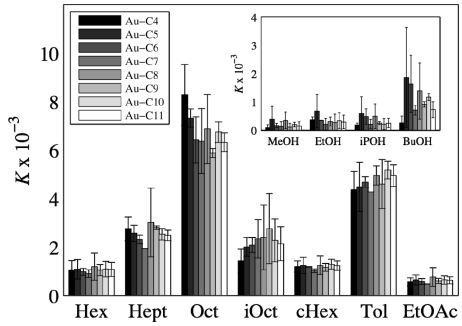

Figure 6. Partition coefficients, *K* ($\times$ 10^{-3}), for all combinations of capped Au nanoparticles and analytes, for $0.0010 \leq P/P^\circ \leq 0.0200$. Each value corresponds to two sensors per Au−C*n*. The inset shows the adjusted *K* values for alcohol vapors.

This type of control is not possible using materials such as carbon black−polymer composites, which contain a random distribution of conductive particles in an insulating matrix. The values of s_{QCM} and *K* did not show a dependence on the chain length of the organic capping ligand, due to the normalization of r_{QCM} by the mass of the capping ligand (eqs 4 and 5). Thus, the uptake of analyte is approximately linear with the mass of the NP ligands. Although larger ligands sorbed more analyte due to a greater amount of ligand mass, the fractional mass change due to analyte sorption was equal for all of the ligands.

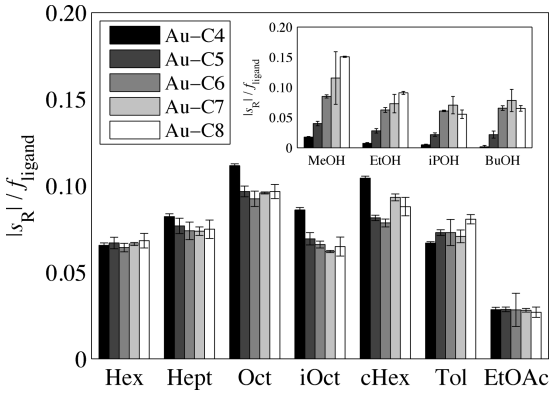

Figure 7. Sensitivity values adjusted by the ligand mass percentage, f_{ligand}, for all sensors and analytes. Each value corresponds to the average of two sensors per Au−C*n*. The inset shows the adjusted s_R values for alcohol vapors.

This observation suggests that all ligands swelled proportionally the same amount for a given $P/P°$ of the analyte vapor.

For hydrocarbons or EtOAc, the sensor sensitivity values, s_R, generally increased monotonically with chain length. For alcohols, the $|s_R|$ values increased with chain length for MeOH and EtOH, however for *i*POH and BuOH, $|s_R|$ values were constant for Au−C6 and longer capping ligands. The resistance response sensitivity to hydrocarbons increased as the length of the capping ligand increased. However, if such sensitivities are adjusted by f_{ligand}, the value of s_R is independent of chain length, as observed for s_{QCM} and the partition coefficients (Figure 7). The purpose of adjusting s_R is to produce a parallel metric to s_{QCM} (i.e., $|s_R|/f_{ligand}$). The observed ΔR values were thus scaled by f_{ligand}, producing s_R values that were independent of chain length. The values of s_R correlated with the relative chain length changes rather than with the absolute change in distance between NPs.

The negative $\Delta R_{max}/R_b$ responses for the alcohol vapors are of note. In general, chemiresistive sorption-based sensors show increases in resistance upon exposure to an analyte. This increase in resistance is normally ascribed to an increase in the separation between the conducting particles (e.g., thiol-capped Au cores) due to swelling of the sensor film upon analyte sorption. Conversely, when negative r_s (i.e., resistance decreases) values are obtained upon exposure to hydrophilic vapors, such behavior is generally associated with a change in the value of ε_s for the metal-to-metal interfacial region. The value of ε_s can be monitored in conjunction with measurement of the plasmon resonance of Au-NPs ($\lambda_{max} \approx 522$ nm).[49,50] An increase of ε_s would cause a red-shift of the plasmon resonance ($\lambda_{max} > 522$ nm). Figure S4 shows the absorption spectra of a Au−C8 film upon exposure to air and to EtOH at $P = P°$, indicating that no significant change in λ_{max} was observed upon exposure to saturated EtOH.

The concentration of analyte sorbed by the sensing material at equilibrium can be calculated by use of the value of K of the analyte/material combination in Figure 6 by

$$K \equiv \frac{C_{A,film}}{C_v} \tag{7}$$

where $C_{A,film}$ (mol L^{-1}) is the concentration of analyte in the film and $C_{A,V}$ (mol L^{-1}) is the concentration of analyte in the vapor phase. The resulting dielectric constant of the analyte-ligand mixture can be calculated by using $C_{A,film}$ (see Appendix A in the Supporting Information). Reynolds et al. demonstrated that an expression describing ε_s for a mixture of two components can be derived:

$$\varepsilon_s = \varepsilon_2 + (\varepsilon_1 - \varepsilon_2)\gamma_1 F_1 \tag{8}$$

where F_1 is assumed to approach unity and γ_1 is the volume ratio of one of the components of the mixture.[51] This determination of γ_1 and K differs from the work of Steinecker et al. in that γ_1 is the volumetric analyte/ligand ratio and K accounts for both the metal core and the passivating ligand.[52] The ε_s value for the ligand is 3.0.[53] At higher values of $C_{A,V}$, higher $\gamma_{analyte}$ should be produced, so ε_s could be significantly affected by the vapor. Figures S5 and S6 show the value of the analyte/ligand mole ratio and the value of ε_s, respectively, as a function of $P/P°$. The value of ε_s is slightly minimized upon exposure to Hex or Tol, whereas for EtOAc and BuOH, ε_s slightly increases. In the case of Hex and Tol, swelling, accompanied by an increase in δ, is expected to dominate the r_S response. For the alcohols, the change in the value of ε_s is about 0.5%, which produces a 0.2% change in λ for $P/P° = 0.0200$ and $\varepsilon_{op} = 1.85$ (i.e., pentane's refractive index, $\eta = 1.36$, $\varepsilon_{op} = \eta^2$).[44] In contrast, the observed change in r_s suggests a 2% change in resistance at $P/P° = 0.0200$ for a Au−C8 sensor upon exposure to BuOH.

Au-NPs that are capped with alkanethiol ligands (e.g., C4−C8) cannot be dissolved in alcoholic solvents, specifically MeOH or EtOH. In fact, EtOH is used to precipitate the particles in solution when using the Brust et al. method.[8] The presence of an alcohol solvent promotes NP aggregation. Exhaustive exposure of a saturated EtOH vapor promotes an irreversible morphology change of a Au−C8 film (Figure S7). The morphology change observed in Figure S7(c) due to EtOH exposure suggests a reduction of the interparticle spacing and an increase in the number of electron hopping pathways. However, for hydrocarbon vapors, NP solvation or swelling occurs. Contrary to significantly changing the value of ε_s, the response data suggests that the negative r_S values are associated with a reversible change in film morphology, as opposed to a change in the value of ε_s. Conversely, an irreversible morphology change was produced when the sensor was heated to 39 °C, as observed in Figure 3.

IV. Conclusions

Au-NPs capped by five different R-SH ligands having variable chain lengths were synthesized and investigated as chemical vapor sensors. The resistance response sensitivity to hydrocarbons increased as the length of the capping ligand increased, whereas for alcohols, negative sensitivities were observed, with increasingly negative sensitivities measured as the length of the capping chain increased. The Au−C*n* sensors with larger ligands sorbed more analyte due to a greater amount of organic mass. The fractional mass change due to analyte sorption was equal for all of the Au−C*n*, suggesting that for any given $P/P°$, all Au−C*n* swelled proportionally the same amount. Consistently, the partition coefficient of all Au−C*n* was approximately equal for every analyte, under the assumption that vapor sorption only occurred in the ligand matrix.

The measurement of partition coefficients of the NP films allowed for estimation of the dielectric constant of the interparticle organic phase upon exposure to the analyte vapor. The dielectric constant change due to sorbed vapor molecules was an order of magnitude lower than what would be needed to

account for the observed resistance responses, suggesting that interparticle distance and/or morphology changes dominate the resistance response. Irreversible morphology changes resulted from heating the Au−C*n* sensors at 40 °C, and the presence of such changes was supported by the change in the sign of the resistance response value upon exposure to EtOH. This observation suggests that the Au−C*n* chemiresistive films can reach a more chemically stable state after such perturbations.

Acknowledgment. The authors thank Carol M. Garland for the TEM measurements. E.G.-B. acknowledges support from the NSF for a graduate fellowship. T.G. and M.E. acknowledge support from Tyco Electronics Corporation. Research was carried out in the Molecular Materials Research Center of the Beckman Institute at Caltech. This work was supported by the NSF, Grant CHE-0604894.

Note Added after ASAP Publication. This article was published ASAP on August 25, 2010. Additional changes have been made throughout the manuscript. The corrected version was published on November 3, 2010.

Supporting Information Available: An appendix is provided describing the calculation of the dielectric constant of the particle-to-particle interface upon analyte exposure. Table S1 shows the values of partial pressure as a function of temperature for *n*-hexane and ethanol. Figure S1 shows a thermogravimetric analysis of Au−C4 and Au−C8. Figure S2 shows the baseline correction of a sensor response. Figure S3 shows the relative differential resistance response as a function of vapor concentration for a Au−C8 sensor. Figure S4 shows optical spectra of a Au NP sensor film upon exposure to air and ethanol. Figure S5 shows the calculated mole ratio as a function of vapor concentration. Figure S6 shows the effective dielectric constant as a function of vapor concentration. Figure S7 shows SEM micrographs of the vapor-treated films. This material is available free of charge via the Internet at http://pubs.acs.org.

References and Notes

(1) Albert, K. J.; Walt, D. R. *Anal. Chem.* **2000**, *72*, 1947–1955.
(2) Severin, E. J.; Doleman, B. J.; Lewis, N. S. *Anal. Chem.* **2000**, *72*, 658–668.
(3) Gao, T.; Woodka, M. D.; Brunschwig, B. S.; Lewis, N. S. *Chem. Mater.* **2006**, *18*, 5193–5202.
(4) Woodka, M. D.; Brunschwig, B. S.; Lewis, N. S. *Langmuir* **2007**, *23*, 13232–13241.
(5) Pearson, R. G. *J. Am. Chem. Soc.* **1963**, *85*, 3533–3539.
(6) Sellers, H.; Ulman, A.; Shnidman, Y.; Eilers, J. E. *J. Am. Chem. Soc.* **1993**, *115*, 9389–9401.
(7) Wohltjen, H.; Snow, A. W. *Anal. Chem.* **1998**, *70*, 2856–2859.
(8) Brust, M.; Walker, M.; Bethell, D.; Schiffrin, D. J.; Whyman, R. J. *J. Chem. Soc., Chem. Commun.* **1994**, 801–802.
(9) Johnson, S. R.; Evans, S. D.; Brydson, R. *Langmuir* **1998**, *14*, 6639–6647.
(10) Woehrle, G. H.; Brown, L. O.; Hutchison, J. E. *J. Am. Chem. Soc.* **2005**, *127*, 2172–2183.
(11) Snow, A. W.; Wohltjen, H. (MicroSensor Systems, Inc.). Materials, Method and Apparatus for Detection and Monitoring of Chemical Species. U.S. Patent 6,221,673, April 24, 2001.
(12) Han, L.; Daniel, D. R.; Maye, M. M.; Zhong, C. *J. Anal. Chem.* **2001**, *73*, 4441–4449.
(13) Joseph, Y.; Besnard, I.; Rosenberger, M.; Guse, B.; Nothofer, H. G.; Wessels, J. M.; Wild, U.; Knop-Gericke, A.; Su, D. S.; Schlogl, R.; Yasuda, A.; Vossmeyer, T. *J. Phys. Chem. B* **2003**, *107*, 7406–7413.
(14) Joseph, Y.; Guse, B.; Yasuda, A.; Vossmeyer, T. *Sens. Actuators, B* **2004**, *98*, 188–195.
(15) Wang, L.; Shi, X.; Kariuki, N. N.; Schadt, M.; Wang, G. R.; Rendeng, Q.; Choi, J.; Luo, J.; Lu, S.; Zhong, C.-J. *J. Am. Chem. Soc.* **2007**, *129*, 2161–2170.
(16) Evans, S. D.; Johnson, S. R.; Cheng, Y. L.; V., S. T. *J. Mater. Chem.* **2000**, *10* (1), 183–188.
(17) Zhang, H. L.; Evans, S. D.; Henderson, J. R.; Miles, R. E.; Shen, T. H. *Nanotechnology* **2002**, *13*, 439–444.
(18) Grate, J. W. *Anal. Chem.* **2003**, *75*, 6759–6759.
(19) Grate, J. W.; Nelson, D. A.; Skaggs, R. *Anal. Chem.* **2003**, *75*, 1868–1879.
(20) Leopold, M. C.; Donkers, R. L.; Georganopoulou, D.; Fisher, M.; Zamborini, F. P.; Murray, R. W. *Faraday Discuss.* **2003**, *125*, 63–76.
(21) Krasteva, N.; Krustev, R.; Yasuda, A.; Vossmeyer, T. *Langmuir* **2003**, *19*, 7754–7760.
(22) Krasteva, N.; Guse, B.; Besnard, I.; Yasuda, A.; Vossmeyer, T. *Sens. Actuators, B* **2003**, *92*, 137–143.
(23) Joseph, Y.; Krasteva, N.; Besnard, I.; Guse, B.; Rosenberger, M.; Wild, U.; Knop-Gericke, A.; Schlogl, R.; Krustev, R.; Yasuda, A.; Vossmeyer, T. *Faraday Discuss.* **2004**, *125*, 77–97.
(24) Zamborini, F. P.; Leopold, M. C.; Hicks, J. F.; Kulesza, P. J.; Malik, M. A.; Murray, R. W. *J. Am. Chem. Soc.* **2002**, *124*, 8958–8964.
(25) Foos, E. E.; Snow, A. W.; Twigg, M. E.; Ancona, M. G. *Chem. Mater.* **2002**, *14*, 2401–2408.
(26) Ahn, H.; Chandekar, A.; Kang, B.; Sung, C.; Whitten, J. E. *Chem. Mater.* **2004**, *16*, 3274–3278.
(27) Briglin, S. M.; Gao, T.; Lewis, N. S. *Langmuir* **2004**, *20*, 299–305.
(28) Guo, J. L.; Pang, P. F.; Cai, Q. Y. *Sens. Actuators, B* **2007**, *120*, 521–528.
(29) Ibañez, F. J.; Zamborini, F. P. *ACS Nano* **2008**, *2*, 1543–1552.
(30) Abeles, B.; Sheng, P.; Coutts, M. D.; Arie, Y. *Adv. Phys.* **1975**, *24*, 407–461.
(31) Joseph, Y.; Peic, A.; Chen, X. D.; Michl, J.; Vossmeyer, T.; Yasuda, A. *J. Phys. Chem. C* **2007**, *111*, 12855–12859.
(32) Brennan, J. L.; Branham, M. R.; Hicks, J. F.; Osisek, A. J.; Donkers, R. L.; Georganopoulou, D. G.; Murray, R. W. *Anal. Chem.* **2004**, *76*, 5611–5619.
(33) Choi, J. P.; Murray, R. W. *J. Am. Chem. Soc.* **2006**, *128*, 10496–10502.
(34) Hicks, J. F.; Zamborini, F. P.; Osisek, A.; Murray, R. W. *J. Am. Chem. Soc.* **2001**, *123*, 7048–7053.
(35) Menard, L. D.; Gao, S. P.; Xu, H. P.; Twesten, R. D.; Harper, A. S.; Song, Y.; Wang, G. L.; Douglas, A. D.; Yang, J. C.; Frenkel, A. I.; Nuzzo, R. G.; Murray, R. W. *J. Phys. Chem. B* **2006**, *110*, 12874–12883.
(36) Parker, J. F.; Choi, J. P.; Wang, W.; Murray, R. W. *J. Phys. Chem. C* **2008**, *112*, 13976–13981.
(37) Terrill, R. H.; Murray, R. W. In *Molecular Electronics*; Ratner, M. A., Jortner, J., Eds.; Blackwell: Oxford, U.K., 1997; pp 215−239.
(38) Terrill, R. H.; Postlethwaite, T. A.; Chen, C. H.; Poon, C. D.; Terzis, A.; Chen, A. D.; Hutchison, J. E.; Clark, M. R.; Wignall, G.; Londono, J. D.; Superfine, R.; Falvo, M.; Johnson, C. S.; Samulski, E. T.; Murray, R. W. *J. Am. Chem. Soc.* **1995**, *117*, 12537–12548.
(39) Wuelfing, W. P.; Murray, R. W. *J. Phys. Chem. B* **2003**, *107*, 6018–6018.
(40) Marcus, R. A.; Sutin, N. *Biochim. Biophys. Acta* **1985**, *811*, 265–322.
(41) Sutin, N. In Electron Transfer in Inorganic, Organic and Biological Systems. *Advances in Chemistry Series 228*; Bolton, J. R., Mataga, N., McLendon, G., Eds.; American Chemical Society: Washington, DC, 1991; Vol. 228, pp 25−43.
(42) Brust, M.; Fink, J.; Bethell, D.; Schiffrin, D. J.; Kiely, C. J. *J. Chem. Soc., Chem. Commun.* **1995**, 1655–1656.
(43) Maldonado, S.; Garcia-Berrios, E.; Woodka, M. D.; Brunschwig, B. S.; Lewis, N. S. *Sens. Actuators, B* **2008**, *134*, 521–531.
(44) *CRC Handbook of Chemistry and Physics*, 77th ed.; CRC Press: New York, 1996−1997.
(45) *Matlab*; MathWorks: Natick, MA, 2009.
(46) Sisk, B. C.; Lewis, N. S. *Sens. Actuators, B* **2003**, *96*, 268–282.
(47) Sauerbrey, G. *Z. Physik.* **1955**, *155*, 206.
(48) Briglin, S. M.; Freund, M. S.; Tokumaru, P.; Lewis, N. S. *Sens. Actuators, B* **2002**, *82*, 54–74.
(49) Templeton, A. C.; Pietron, J. J.; Murray, R. W.; Mulvaney, P. *J. Phys. Chem. B* **2000**, *104*, 564–570.
(50) Underwood, S.; Mulvaney, P. *Langmuir* **1994**, *10*, 3427–3430.
(51) Reynolds, J. A.; Hough, J. M. *Proc. Phys. Soc., London, Ser. B* **1957**, *70*, 769–775.
(52) Steinecker, W. H.; Rowe, M. P.; Zellers, E. T. *Anal. Chem.* **2007**, *79*, 4977–4986.
(53) Hicks, J. F.; Templeton, A. C.; Chen, S. W.; Sheran, K. M.; Jasti, R.; Murray, R. W.; Debord, J.; Schaaf, T. G.; Whetten, R. L. *Anal. Chem.* **1999**, *71*, 3703–3711.

JP101331G